

**Dynamic Pavement Response
Measurement System using
Piezoelectric Axle Sensors**

**A Thesis Submitted to the College of
Graduate Studies and Research
in Partial Fulfillment of the Requirements
for the Degree of Master of Science
in the Department of Electrical Engineering
University of Saskatchewan
Saskatoon, Saskatchewan, Canada**

G469
Oct. 1/02
JAH

by

Rebecca Jean Huff

Fall 2002

PERMISSION TO USE

In presenting this thesis in partial fulfillment of the requirements for a Postgraduate degree from the University of Saskatchewan, I agree that the Libraries of this University may make it freely available for inspection. I further agree that permission for copying of this thesis in any manner, in whole or in part, for scholarly purposes may be granted by the professor or professors who supervised my thesis work or, in their absence, by the Head of the Department or the Dean of the College in which my thesis work was done. It is understood that any copying or publication or use of this thesis or parts thereof for financial gain shall not be allowed without my written permission. It is also understood that due recognition shall be given to me and to the University of Saskatchewan in any scholarly use which may be made of any material in my thesis.

Requests for permission to copy or to make other use of material in this thesis in whole or part should be addressed to:

Head of the Department of Electrical Engineering
College of Engineering, 57 Campus Drive
University of Saskatchewan
Saskatoon, Saskatchewan, Canada
S7N 5A9

UNIVERSITY OF SASKATCHEWAN

**Dynamic Pavement Response
Measurement System using
Piezoelectric Axle Sensors**

Candidate: Rebecca Huff

Supervisor: B.L.F. Daku
Supervisor: C.F. Berthelot

M.Sc. Thesis Submitted to the
College of Graduate Studies and Research

Fall, 2002

ABSTRACT

Over the past several decades, the transportation of commercial goods in North America has shifted from using railways to using roadways. This came as a result of the recent development of high quality roads reaching the same destinations as the railroads'. Historically, roadway design has used an empirical approach. Essentially, this technique was adequate in dealing with small vehicles and low volumes of traffic.

Today, however, large vehicles and high traffic volumes are inflicting increasing amounts of damage on many roadways. As such, the idea of developing a mechanistic road modeling approach for design, construction and preservation was conceived. The ability to determine the Dynamic Deflection Bowl surrounding a rolling wheel is required for the prediction of structural damage.

This thesis presents the Piezoelectric Axle Sensor (PAS) as a possible tool for obtaining the Dynamic Deflection Bowl information. It is a sensor which converts mechanical deformation into a proportional electrical charge, and there are already thousands of these sensors installed in systems world wide, measuring the Dynamic Weights of vehicles. The operation of several different types and orientations of these PAS's were examined and tested. Valuable data was extracted from their outputs. This data allowed the prediction of many, but not all, of the Deflection Bowl characteristics.

For instance, the length and inflection point of the Deflection Bowl along with footprint size were all successfully predicted. The horizontal and vertical components for the two pseudo-rectangular PAS's were combined and found to exhibit the same characteristics as the cylindrical PAS. This research has shown that the outputs from several popular PAS's can be used to generate data useful in planning and maintenance of the nations roadways.

ACKNOWLEDGEMENTS

It is my pleasure to recognize, with utmost appreciation, all those who have helped in making my research a success. In particular, many thanks to both of my supervisors, Dr. Brian Daku and Dr. Curtis Berthelot. Dr. Daku is an Electrical Engineering Professor at the University of Saskatchewan, whose excellent assistance provided a good foundation for, and continual support throughout, the writing of this thesis. Dr. Berthelot is a Civil Engineer in the Transportation Research Center at the University of Saskatchewan, who not only identified the problems that formed the basis of my research, but was extremely helpful in discussing and evaluating possible strategies to solve them, and ultimately showed me that nothing was impossible.

Likewise, I gratefully acknowledge the support of Mr. Ron Koenderink, Chief Engineer at International Road Dynamics Inc., who was also extremely instrumental in problem identification and was always available to consider and assess various approaches.

This Master of Science project in Electrical Engineering was pursued in collaboration with Telecommunication Research Laboratories (TRLabs), International Road Dynamics Inc. (IRD), the Transportation Research Center at the University of Saskatchewan, and the Department of Highways and Transportation, a department within the Government of Saskatchewan - whom all have been very supportive with funding, in-kind contributions, and continual assistance.

Credit is also due to the Highway Crews and IRD Roadies that did the installation!

Moreover, thank-you is extended to my colleagues for lending an ear and offering suggestions from time to time.

I conclude by sending a special thanks to my close friends and family, especially my parents Bev and Jerry Huff who have been by my side throughout. Without their tremendous love and support, I would not be where I am today.

Thank you...

To my parents, with love
R.J.H.

TABLE OF CONTENTS

PERMISSION TO USE	i
ABSTRACT	ii
ACKNOWLEDGEMENTS.....	iii
TABLE OF CONTENTS.....	v
LIST OF TABLES	ix
LIST OF FIGURES	xi
LIST OF ABBREVIATIONS.....	xvii
1 Introduction	1
1.1 Proposed Approach to Measure Surface Deflection.....	5
1.2 Research Objectives.....	8
1.3 Applications	8
1.4 Scope.....	9
1.5 Organization of Thesis	10
2 Theoretical Concepts.....	11
2.1 Deflection Bowl Background Theory and Modeling.....	11
2.1.1 Static Deflection Bowl Theory	12
2.1.2 Dynamic Deflection Bowl Theory.....	14
2.2 Piezoelectricity Background Theory and Modeling	18
2.2.1 Theory and Modeling.....	19
2.2.2 Fabrication of Sensors	20
2.2.3 Principle of Operation.....	20
2.2.4 Loading Assumptions	26
2.2.5 Signal Conditioning	27
2.2.6 Differentiating Signal from Noise	27
2.3 Various PAS Models and Theoretical Results.....	28
2.3.1 Thermocoax Vibracoax (8 mm Bare)	29
2.3.2 Thermocoax Vibracoax (3 mm Encapsulated)	29

2.3.3	MSI Roadtrax BL (Normal).....	30
2.3.4	MSI Roadtrax BL (Rotated 90°).....	31
2.4	Background on Stresses Applied to the Sensor and Expected PAS Response ...	32
2.4.1	Theoretical Thermo-B Sensor Output.....	33
2.4.2	Theoretical MSI Sensor Output	35
2.4.3	Theoretical MSI90 Sensor Output	36
2.4.4	Dependency on Size of Sensing Area.....	38
3	System Design Details	39
3.1	Test Section Selection.....	39
3.2	System Overview	41
3.3	System Design Process	42
3.4	Installation of System and Explanation of System Settings	44
4	Data Collection	62
4.1	General Information.....	62
4.2	Dynamic Weight (WIM) Data & Statistical Analysis	65
4.2.1	Statistical Representation of WIM Data	69
4.2.2	Adjusted System Settings for Proper Calibration	70
4.2.3	Selecting a Pass from each Set to be used for Further Analysis.....	75
4.3	Temperature Data.....	77
4.3.1	Calculation of Temperature from A/D output values	77
4.4	Deflection Bowl Data & Statistical Analysis.....	78
4.4.1	Statistical Analysis of Benkelman Beam Data	80
4.5	PAS Data & Statistical Analysis.....	82
4.5.1	Statistical Analysis of PAS Data	86
5	Results and Discussion	89
5.1	Deflection Bowl Data Interpretation.....	89
5.2	PAS Data Interpretation	92
5.2.1	Calculation of Distance per Sample for Set _{80km/h} and Set _{60km/h}	92
5.2.2	Comparison of PAS Response Signals for the Two Separate Sets.....	96
5.2.3	Detailed Explanation of different Regions of the PAS Response Signal ..	100

5.2.4	Using the PAS Response to Determine Footprint Dimensions	105
5.3	Shifting & Summation of MSI90 and MSI to get Thermo-B data	107
5.3.1	Shifting the MSI90 and MSI Signals	108
5.3.2	Summing the MSI90 and MSI signals	111
5.3.3	Comparison between the Summation of the MSI90 and MSI PAS's to the Response of the Thermo-B PAS	114
5.3.4	Possible Explanation for Differences between Cylindrical PAS output and Summation of the Two MSI outputs	115
5.4	Comparison of Deflection Bowl Data and PAS Data	116
5.4.1	Methodology for Correlation	116
5.4.2	Results and Discussion	117
6	Conclusion	122
6.1	Summary	122
6.2	Discussion	122
6.3	Results	125
6.4	Further Recommendations & Future Research	126
REFERENCES		128
A	Data Sheets	131
B	Site Layout Diagram	166
C	Data Collection Instructions	168
C.1	General Information (How to open/change b/t screens in Unix)	168
C.2	General Data Collection Requirements	168
C.3	Collecting WIM Data	168
C.4	Collecting PAS Data	169
C.5	Converting PAS Data	169
C.6	Saving PAS Data	170
C.7	Saving WIM Data	170
D	Raw WIM Data	171
E	Raw LM35 Temperature Data	174

F	Raw Benkelman Beam Data.....	176
G	Raw PAS Data	183
H	PAS Data vs. Deflection Bowl Data	205
I	Calculations.....	208
I.1	Chapter 3 (Section 3.4)	208
I.2	Chapter 4 (Section 4.2.1)	208
I.3	Chapter 4 (Section 4.3.1)	209
I.3.1	Calculation of Temperature from A/D output values	209
I.4	Chapter 5 (Section 5.2.1)	211
I.4.1	Calculation of Distance per Sample for Set _{80km/h}	211
I.5	Chapter 5 (Section 5.3.2)	213

LIST OF TABLES

Table 2.1	All PAS Models with Corresponding Part Numbers	28
Table 4.1	Actual Benkelman Beam Static Truck Information.....	63
Table 4.2	Weather Conditions for Wednesday April 18 th , 2001.....	64
Table 4.3	WIM System Electronics Threshold & Calibration Settings for Set _{80km/h} & Set _{60km/h}	66
Table 4.4	WIM System Electronics Compiled Raw Data for Set _{80km/h} & Set _{60km/h}	67
Table 4.5	Correction Factors and New Calibration Factors – Set _{80km/h} & Set _{60km/h}	71
Table 4.6	Dynamic Weights Calculated using New Calibration Factors (for all Passes).....	73
Table 4.7	Differences between Static Weights and actual measured Dynamic Weights	76
Table 4.8	Conversion of Digital values to Actual Voltages	77
Table 4.9	Pavement Temperatures calculated for all 20 Passes	78
Table 4.10	Deflection Measurement vs. Distance	79
Table 4.11	Length and Maximum Depth for each Static Benkelman Beam Deflection Bowl and Statistical Analysis Results for all Benkelman Beam Data.....	81
Table 4.12	Back Axle Zero Crossing Points (Pass #16).....	83
Table 4.13	Number of Zeros added to line up different data sets & New Starting Points (Pass #16).....	83
Table 4.14	Statistical Analysis Results for Thermo-E (Pass 1-10).....	88
Table 5.1	Summary of distance/sample for both Sets.....	96
Table 6.1	Comparison of Theoretical and Test PAS Responses.....	124
Table D.1	WIM System Electronics Dynamic Back Axle Weights and Axle Spacings for Set _{80km/h}	172
Table D.2	WIM System Electronics Dynamic Back Axle Weights and Axle Spacings for Set _{60km/h}	172

Table D.3	Dynamic Weights calculated using New Calibration Factors (for all Passes).....	173
Table F.1	Benkelman Beam data Bowls (Raw data from SK. Highways)	176
Table F.2	Bowl #1 (Thermo-E).....	178
Table F.3	Summary Length, Max. Depth and Area for Bowl#1 (Thermo-E).....	178
Table F.4	Bowl#2 (Thermo-B)	179
Table F.5	Summary of Length, Max. Depth and Area for Bowl#2 (Thermo-B).....	179
Table F.6	Bowl#3 (Pavement)	180
Table F.7	Summary of Length, Max. Depth and Area for Bowl#3 (Pavement).....	180
Table F.8	Bowl#4 (MSI90).....	181
Table F.9	Summary of Length, Max. Depth and Area for Bowl#4 (MSI90).....	181
Table F.10	Bowl#5 (MSI).....	182
Table F.11	Summary of Length, Max. Depth, and Area for Bowl#5 (MSI)	182
Table G.1	Determination of # of Zeroes and Starting Point needed to Shift Data.	187
Table G.2	Statistical Analysis for Thermo-E (Pass 1-10)	196
Table G.3	Statistical Analysis for Thermo-B (Pass 1-10)	198
Table G.4	Statistical Analysis for MSI90 (Pass 1-10).....	200
Table G.5	Statistical Analysis for MSI (Pass 1-10).....	202
Table I.1	Conversion of Digital values to Actual Voltages	209

LIST OF FIGURES

Figure 1.1	Top, Front, and Side Views of a Deflection Bowl.....	2
Figure 1.2	Benkelman Beam Measurement Technique	3
Figure 1.3	Falling Weight Deflectometer Measurement Technique.....	4
Figure 1.4	Multi-Depth Deflectometer Measurement Technique.....	5
Figure 1.5	Top View of an Axle Passing Over a Piezoelectric Axle Sensor.....	5
Figure 1.6	Piezoelectric Axle Sensor Response to a Dynamic Load (Output signal, from the previous Figure 1.5, as the tire approaches, passes over, and departs from the PAS).....	6
Figure 2.1	Road Structure Cross Section	11
Figure 2.2	Deflection Bowl Around a Static Load.....	12
Figure 2.3	Strain vs. Time as a result of a constant Stress for a Visco-elastic material such as HMAC.....	13
Figure 2.4	Spring Model of Road Infrastructure (Elastic Material Characteristics).....	14
Figure 2.5	Spring/Dash-Pot Model of Road Infrastructure (Visco-elastic Material Characteristics)	15
Figure 2.6	Stress vs. Strain Curve for Steel	15
Figure 2.7	Stress vs. Strain Curve for HMAC	16
Figure 2.8	Inelastic vs. Elastic Systems of Roads.....	17
Figure 2.9	Tension and Compression Components Exerted on the Road Surface	17
Figure 2.10	Deflection of a Piezoelectric Element	19
Figure 2.11	Charge Model for a Piezoelectric Sensor	21
Figure 2.12	Ideal Charge Model for PAS	21
Figure 2.13	Currents and Voltages as a result of a Step Change Input.....	22
Figure 2.14	Currents and Voltages as a result of a Gradual Linear Input.....	23
Figure 2.15	Axle with Dual Radial Tires	26

Figure 2.16 Thermocoax Vibracoax (8 mm Bare) - Shown Installed.....	29
Figure 2.17 Thermocoax Vibracoax (3 mm Encapsulated) - Shown Installed	30
Figure 2.18 (a) Stress Applied to Largest Dimension (b) Stress Applied to Thinnest Dimension.....	30
Figure 2.19 MSI Roadtrax BL (Normal) – Shown Installed.....	31
Figure 2.20 MSI Roadtrax BL (Tilted 90) – Shown Installed	31
Figure 2.21 Theoretical Vertical and Horizontal Deflection as seen by point P.....	32
Figure 2.22 Theoretical Voltage and Current output signals from a Thermo-B PAS.....	34
Figure 2.23 Deflection as seen by the MSI PAS (NOT TO SCALE).....	35
Figure 2.24 Theoretical Voltage and Current output signals from a MSI PAS	36
Figure 2.25 Deflection as seen by the MSI90 PAS.....	37
Figure 2.26 Theoretical Voltage and Current output signals from a MSI90 PAS	37
Figure 2.27 Theoretical PAS output signals (current) as a result of changes in Sensing Area	38
Figure 3.1 Partial Site Layout Diagram	40
Figure 3.2 Block diagram of System Overview	41
Figure 3.3 Sensing System Block Diagram	42
Figure 3.4 Data Acquisition System Block Diagram.....	44
Figure 3.5 Trenching and Installing the Conduits.....	45
Figure 3.6 Backfilling the Trenches.....	45
Figure 3.7 Marking the Road	46
Figure 3.8 Cutting the Road	46
Figure 3.9 Inductive Loop Installation.....	47
Figure 3.10 Sensor Preparation	47
Figure 3.11 Sensor Installation (1 out of 4)	48
Figure 3.12 Trenching again to Match Sensor Leads to Conduits.....	48

Figure 3.13 Routing Cables Through Conduit.....	49
Figure 3.14 Splice Cables.....	50
Figure 3.15 System Electronics.....	51
Figure 3.16 Threshold Value.....	55
Figure 3.17 Calibration Factor	58
Figure 3.18 Whole System and External Housing	61
Figure 4.1 Benkelman Beam Truck gathering Deflection Bowl Measurements	63
Figure 4.2 Summarized Dynamic Weights calculated by WIM for Passes 1-20	68
Figure 4.3 Dynamics Weights calculated using New Calibration Factors [Passes 1-20].....	74
Figure 4.4 This is the same as Figure 4.3 but without MSI 90 Sensor	74
Figure 4.5 Benkelman Beam Deflection Measurement vs. Distance for all 5 Deflection Bowls	80
Figure 4.6 Average Deflection Bowl Data.....	81
Figure 4.7 Pass #16 Raw PAS data for all sensors	82
Figure 4.8 Pass #16 Processed PAS data for all sensors (inverted, zeroed and adjusted).....	84
Figure 4.9 Processed PAS data but only for the Back Axle (Pass #16).....	84
Figure 4.10 Processed PAS Data (Concentrating on the Peaks and Zero Crossings).....	85
Figure 4.11 All Passes (2-10) for Thermo-E (Sample Number 2900-3100).....	87
Figure 4.12 All Passes (2-10) for Thermo-E (Sample Number 2650-3450).....	87
Figure 5.1 Average Deflection Bowl data along with its Corresponding Trendline.....	90
Figure 5.2 Partially Processed Thermo-B data Pass #16	93
Figure 5.3 Processed PAS data Pass #16 (All Sensors)	95
Figure 5.4 Comparison of Thermo-E PAS (Pass #6 & Pass #16).....	98
Figure 5.5 Comparison of Thermo-B PAS (Pass #6 & Pass #16).....	98
Figure 5.6 Comparison of MSI90 PAS (Pass #6 & Pass #16).....	99

Figure 5.7 Comparison of MSI PAS (Pass #6 & Pass #16)	100
Figure 5.8 Back Axle of the Partially Processed Thermo-B	101
Figure 5.9 Back Axle of the Thermo-B (Sample Numbers 1200-1408).....	102
Figure 5.10 Back Axle of the Thermo-B (Sample Numbers 1408-1605).....	102
Figure 5.11 Back Axle of the Thermo-B (Sample Numbers 1605-1671).....	103
Figure 5.12 Back Axle of the Thermo-B (Sample Numbers 1671-1694).....	103
Figure 5.13 PAS Response due to the Approach of the Vehicle (1408-1694).....	104
Figure 5.14 Back Axle of the Thermo-B (Sample Numbers 1671-1723).....	106
Figure 5.15 Original PAS Output data for Pass #16	109
Figure 5.16 Back Axle of Truly Shifted data	111
Figure 5.17 Raw PAS data for MSI90 and MSI	113
Figure 5.18 Normalized Resultant Current for Summation of MSI90 and MSI PASs..	114
Figure 5.19 MSI90 and MSI Normalized Summation Superimposed on the Thermo- B Normalized Absolute Value Waveform.....	115
Figure 5.20 MSI90 PAS Data with Benkelman Beam Data Superimposed	118
Figure 5.21 MSI90 PAS data vs. Benkelman Beam data.....	119
Figure 5.22 MSI90 PAS with Benkelman Beam data Superimposed (showing specific points of interest).....	120
Figure B.1 Site Layout Diagram.....	167
Figure E.1 Raw LM35 Temperature Sensor Data for All Passes	174
Figure E.2 Raw LM35 Temperature Sensor Data for Passes 1-10.....	175
Figure E.3 Raw LM35 Temperature Sensor Data for Passes 11-20.....	175
Figure F.1 Bowl #1 (Thermo-E).....	178
Figure F.2 Bowl#2 Thermo-B	179
Figure F.3 Bowl#3 (Pavement)	180
Figure F.4 Bowl#4 (MSI90)	181

Figure F.5 Bowl#5 (MSI).....	182
Figure G.1 Raw PAS Data for Pass #1 (left), Pass #2 (right).....	183
Figure G.2 Raw PAS Data for Pass #3 (left), Pass #4 (right).....	183
Figure G.3 Raw PAS Data for Pass #5 (left), Pass #6 (right).....	184
Figure G.4 Raw PAS Data for Pass #7 (left), Pass #8 (right).....	184
Figure G.5 Raw PAS Data for Pass #9 (left), Pass #10 (right).....	184
Figure G.6 Raw PAS Data for Pass #11 (left), Pass #12 (right).....	185
Figure G.7 Raw PAS Data for Pass #13 (left), Pass #14 (right).....	185
Figure G.8 Raw PAS Data for Pass #15 (left), Pass #16 (right).....	185
Figure G.9 Raw PAS Data for Pass #17 (left), Pass #18 (right).....	186
Figure G.10Raw PAS Data for Pass #19 (left), Pass #20 (right).....	186
Figure G.11Zoomed in on Raw PAS Data (Pass #2).....	189
Figure G.12Zoomed in on Raw PAS Data (Pass #3).....	189
Figure G.13Zoomed in on Raw PAS Data (Pass #4).....	190
Figure G.14Zoomed in on Raw PAS Data (Pass #5).....	190
Figure G.15Zoomed in on Raw PAS Data (Pass #6).....	190
Figure G.16Zoomed in on Raw PAS Data (Pass #7).....	191
Figure G.17Zoomed in on Raw PAS Data (Pass #8).....	191
Figure G.18Zoomed in on Raw PAS Data (Pass #9).....	191
Figure G.19Zoomed in on Raw PAS Data (Pass #10).....	192
Figure G.20Zoomed in on Raw PAS Data (Pass #11).....	192
Figure G.21Zoomed in on Raw PAS Data (Pass #12).....	192
Figure G.22Zoomed in on Raw PAS Data (Pass #13).....	193
Figure G.23Zoomed in on Raw PAS Data (Pass #14).....	193
Figure G.24Zoomed in on Raw PAS Data (Pass #15).....	193

Figure G.25	Zoomed in on Raw PAS Data (Pass #16)	194
Figure G.26	Zoomed in on Raw PAS Data (Pass #17)	194
Figure G.27	Zoomed in on Raw PAS Data (Pass #18)	194
Figure G.28	Zoomed in on Raw PAS Data (Pass #19)	195
Figure G.29	Zoomed in on Raw PAS Data (Pass #20)	195
Figure G.30	All Passes (2-10) for Thermo-B (Sample Number 2900-3100)	197
Figure G.31	All Passes (2-10) for Thermo-B (Sample Number 2650-3450)	197
Figure G.32	All Passes (2-10) for MSI90 (Sample Number 2900-3100)	199
Figure G.33	All Passes (2-10) for MSI90 (Sample Number 2650-3450)	199
Figure G.34	All Passes (2-10) for MSI (Sample Number 2900-3100)	201
Figure G.35	All Passes (11-20) for MSI (Sample Number 2650-3450)	201
Figure G.36	All Passes (11-20) for Thermo-E (Sample Number 2900-3100 & 2650-3450)	203
Figure G.37	All Passes (11-20) for Thermo-B (Sample Number 2900-3100 & 2650-3450)	203
Figure G.38	All Passes (11-20) for MSI90 (Sample Number 2900-3100 & 2650-3450)	203
Figure G.39	All Passes (11-20) for MSI (Sample Number 2900-3100 & 2650-3450)	204
Figure H.1	(a) Thermo-E PAS and Benkelman Beam data plotted Simultaneously (b) Thermo-E PAS data vs. Benkelman Beam data	205
Figure H.2	(a) Thermo-B PAS and Benkelman Beam data plotted Simultaneously (b) Thermo-B PAS data vs. Benkelman Beam data	206
Figure H.3	(a) MSI PAS and Benkelman Beam data plotted Simultaneously (b) MSI PAS data vs. Benkelman Beam data	207
Figure I.1	Bell Curves depicting small and large St. Dev's	209
Figure I.2	Partially Processed Thermo-B data Pass #6	211
Figure I.3	Processed PAS data Pass #6 (All Sensors)	213
Figure I.4	Vector Addition	214

LIST OF ABBREVIATIONS

A/D	Analog to Digital Converter
BL	Brass Linguini
CV	Coefficient of Variation
DCF	Dynamic Compensation Factor
D84011	Benkelman Beam Truck Number
FWD	Falling Weight Deflectometer
GNP	Gross National Product
H/D	Hard Drive
HMAC	Hot Mix Asphalt Concrete
I/F	Interface
IRD	International Road Dynamics Inc.
LM35	Precision Centigrade Temperature Sensor
LVDT	Linear Variable Differential Transducer/Transformer
MDD	Multi-Depth Deflectometer
MSI	Measurement Specialties Inc. – Roadtrax BL PAS
MSI90	Measurement Specialties Inc. – Roadtrax BL (Tilted 90°) PAS
PAS	Piezoelectric Axle Sensor
PCL-818H	A/D Card
POC	Point of Contact
PVC	Polyvinyl Chloride
PVdf	Polyvinylidene Fluoride
St. Dev.	Standard Deviation
Thermo-B	Thermocoax - Vibracoax (8mm Bare) Piezoelectric Axle Sensor
Thermo-E	Thermocoax - Vibracoax (3mm Encapsulated) Piezoelectric axle Sensor
TL082	Operational Amplifier
TRLabs	Telecommunication Research Laboratories
WIM	Weigh-In-Motion

1 Introduction

The gross national product (GNP) of a particular country is a strong function of the efficiency of that country's transportation infrastructure. It is only during the last 40 years that there have been high quality roads that reach all of the same communities and destinations that the railroads have historically served. In contrast to railroads, trucks, with the ability to operate economically on short runs, have considerable scheduling flexibility. This allows the convenience of 'door to door' and 'just-in-time' delivery of goods [1].

In the past several decades, there has been a major shift in rural transportation from rail to road, resulting in significant increases in load related damage to the road infrastructure. In addition, due to the increase in allowable axles and gross vehicle weights on roadways, commercial trucks are now permitted to be bigger and carry larger loads than ever before, causing additional damage to roadways [2].

Saskatchewan, for example, has been noted for being at the forefront in the development of new road and trucking technology. The province works in partnership with industry and universities to develop new trucking technologies. For instance, air-spring and dynamic tuned suspension systems are essential developments of this type of technological advancement. Generally, these measures have enhanced safety and efficiency. Moreover, they have minimized, but not eliminated, damage inflicted on the road infrastructure as a result of dynamic loading effects.

As such, the Government of Saskatchewan co-operates with the trucking industry to create a positive environment that enables this industry to offer service as efficiently as

possible, providing due regard to the safety of the motoring public and the preservation of the publicly owned highway infrastructure [3].

The physical damage inflicted on the road is related to the surface deflection in the pavement due to loading. Each vehicle tire surface that touches the road creates some surface deflection. This deflection (road structure response to static/dynamic loading) in the vicinity of the tire is referred to as a "Deflection Bowl", and is illustrated in Figure 1.1.

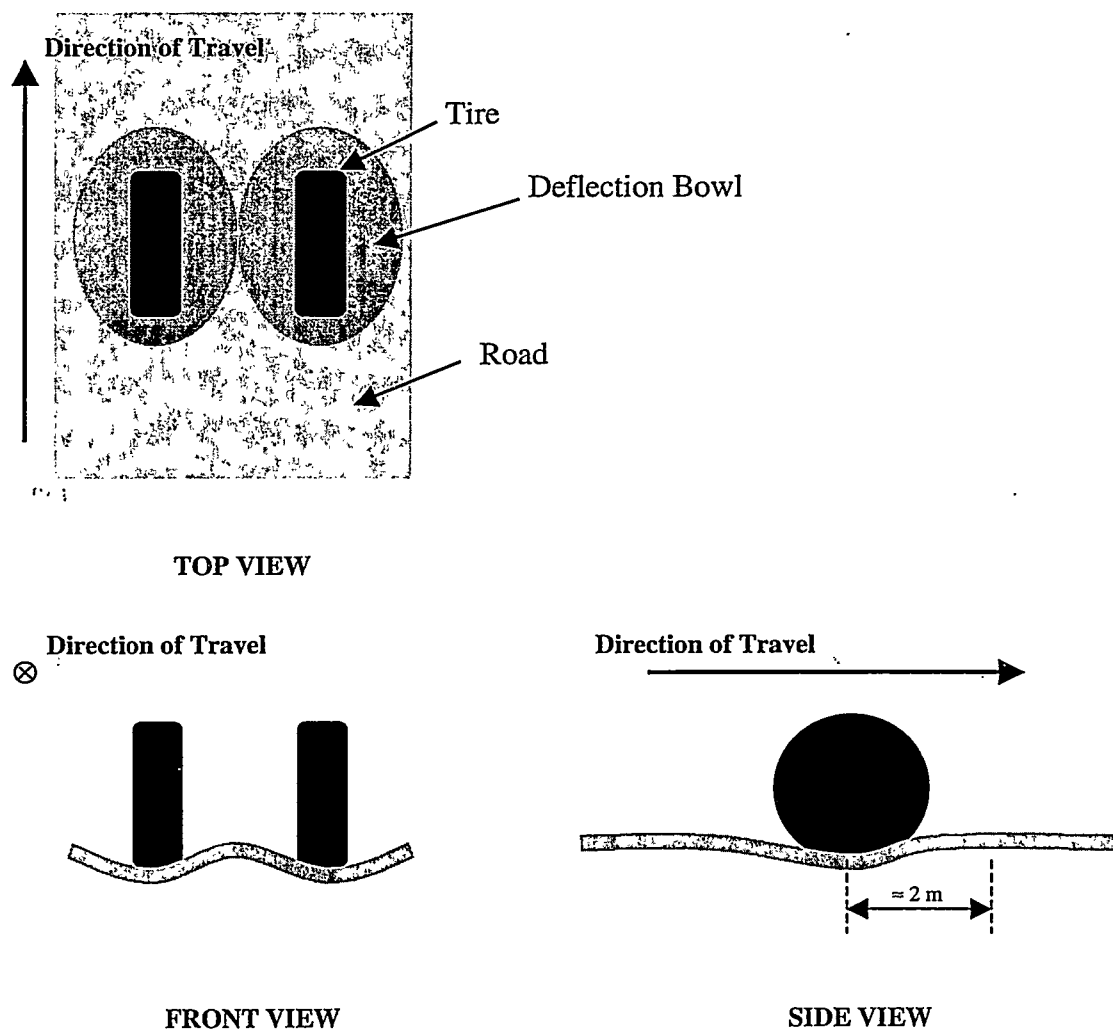


Figure 1.1 Top, Front, and Side Views of a Deflection Bowl

This figure shows that road deformation starts to occur at some distance in advance of the actual tire to pavement contact area - approximately 2 m for the average commercial truck on a Hot Mix Asphalt Concrete road structure. This distance varies with respect to material properties and thickness' of the road, size of the tire, and degree of loading. If the surface deflection does not fully recover, pavement damage has occurred. Cumulative pavement damage will eventually result in road failure.

In the past, Departments of Highways have typically measured this surface deflection on roadways using instruments and techniques such as the Benkelman Beam, the Falling Weight Deflectometer (FWD), and the Multi-Depth Deflectometer (MDD). Basically, these instruments and techniques have been developed to measure surface deflection in an attempt to characterize deterioration of roadways. The Benkelman Beam technique is capable of yielding accurate static surface deflection results, but it cannot obtain the dynamic measurement. It is also dangerous because it requires a team of persons on the roadway to obtain these measurements. The tip of the beam, shown in Figure 1.2, is initially placed perpendicular to the tire at its center point and the Recording Dial Gauge is set to zero. Manual readings are taken every 10 cm, by an operator lying on the surface of the road, as the Benkelman Beam truck pulls away from the tip of the beam.

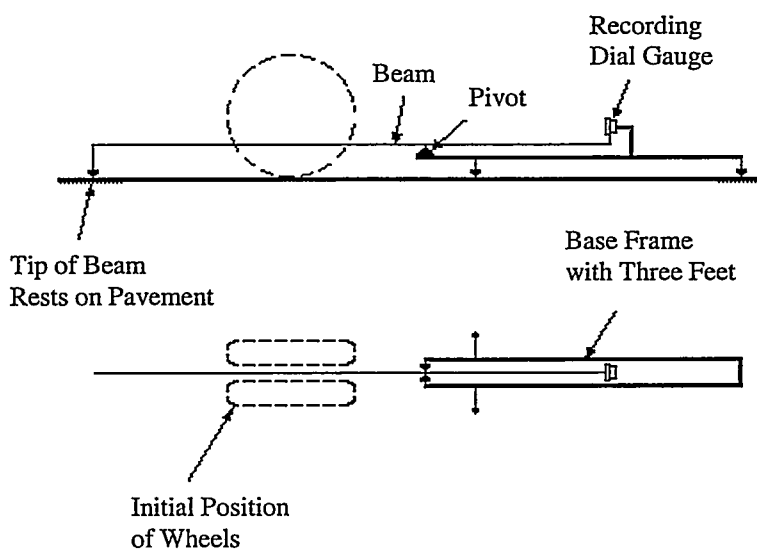


Figure 1.2 Benkelman Beam Measurement Technique

The FWD technique is, conversely, capable of simulating and measuring effects of dynamic loading. As the weight drops, the spring system (visco-elastic damper) shown in Figure 1.3, is engineered to simulate a passing wheel load while data is recorded from the geophones. Although it still cannot give a response to an actual moving vehicle - only a simulation of such - it does however, have the advantage of being portable and through back-calculation techniques it is capable of determining material properties.

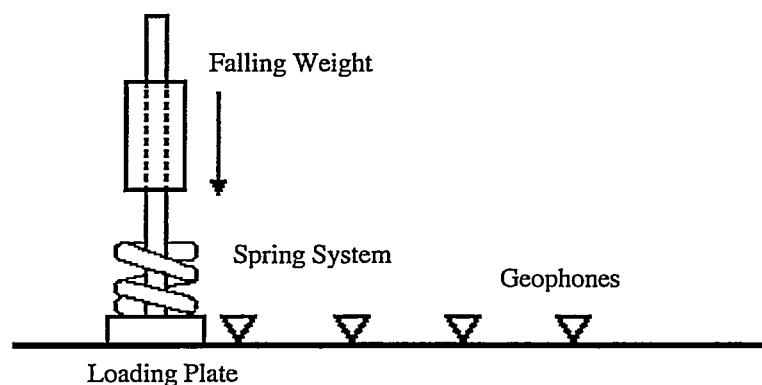


Figure 1.3 Falling Weight Deflectometer Measurement Technique

A system that is capable of dynamic measurements, such as “in-situ” elastic deflections and (or) permanent deformations in multiple pavement layers, is the MDD. The MDD consists of a series of Linear Variable Differential Transducers (LVDT). As the vehicle travels over the sensor, the pavement deflects under the wheel load. This deflection will cause the series of LVDT’s, anchored to the sides of the hole, to move with respect to the 3 m stationary rod (anchored into the subgrade), as shown in Figure 1.4. These sensors work magnetically on the principle of a transformer with a variable coupling coefficient. The LVDT’s movement (displacement) is recorded - as a voltage - with respect to the location of ferrous metal “slugs” in the center rod. Although there is damage to the road caused by drilling this 3.81 cm (1.5”) vertical hole during installation, a more significant reason this technique is not widely accepted for determining surface deflection, is because of its excessive cost and lack of portability.

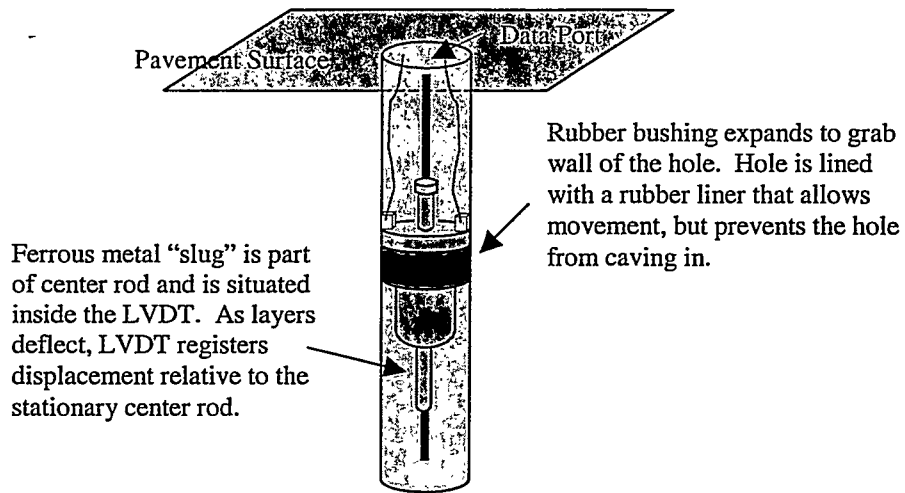


Figure 1.4 Multi-Depth Deflectometer Measurement Technique

1.1 Proposed Approach to Measure Surface Deflection

Around the world, commercial trucks are monitored for planning, design, and preservation requirements by Highway Departments using Intelligent Transportation Systems, such as Weigh-In-Motion (WIM) systems (i.e., dynamic weighing of vehicles). Many of these WIM installations (sensor configurations) use piezoelectric sensors in combination with other vehicle sensing technologies that are installed directly into the surface of the roadway, across the width of each lane. These sensors are called Piezoelectric Axle Sensors (PAS) since both tires of each axle cross the sensor at the same time, as shown in Figure 1.5.

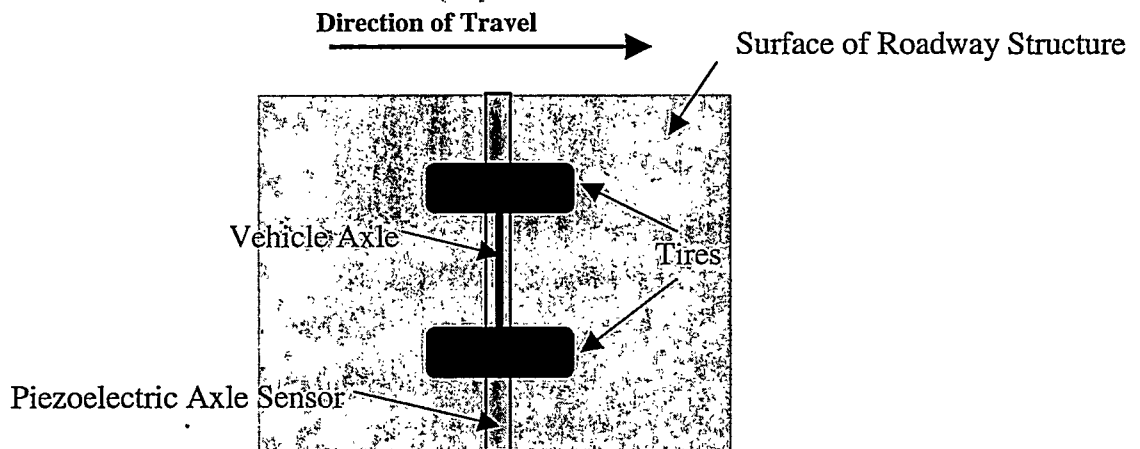


Figure 1.5 Top View of an Axle Passing Over a Piezoelectric Axle Sensor

The outputs from these sensors provide the input to a set of System Electronics comprised of a Data Acquisition System used to acquire, analyze, and through calculations, determine the Dynamic Weight of each passing vehicle. The Dynamic Weight of a vehicle is time varying because of accelerations induced to the wheel by irregularities in the road surface. The vehicle suspension also plays a part in this situation. This Dynamic Weight oscillates around the Static Weight of the vehicle. The output of the PAS is used to calculate this instantaneous weight (point on the oscillating output). This calculated instantaneous weight consists of a dynamic component and a system error component due to the sensor itself and the electronics supporting the sensor.

An example of a signal from a PAS, after partial processing (one level of integration), is shown in Figure 1.6. This particular processed version of the raw data was chosen because it is used to directly calculate the Dynamic Weight. This signal has three very different and distinct regions which are labeled A, B, and C.

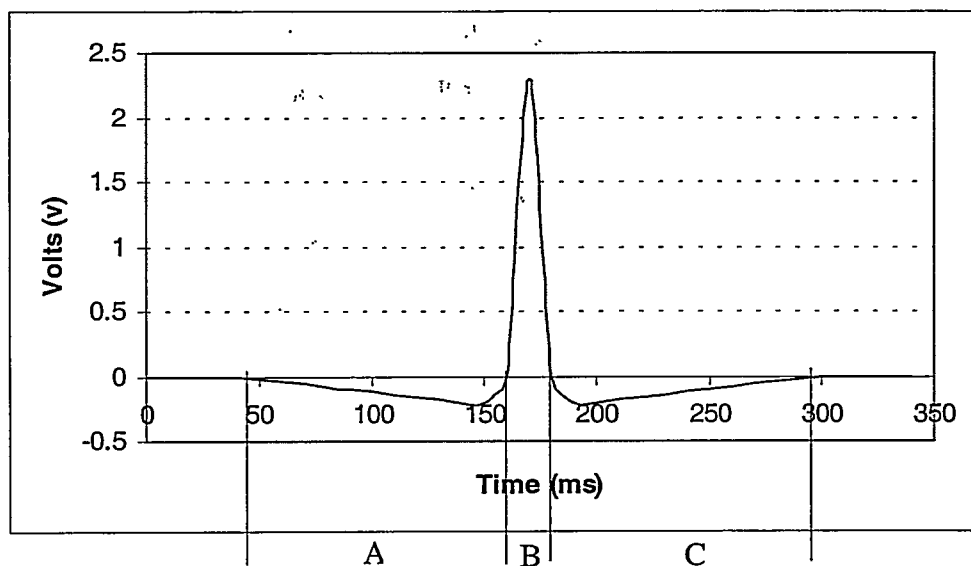


Figure 1.6 Piezoelectric Axle Sensor Response to a Dynamic Load (Output signal, from the previous Figure 1.5, as the tire approaches, passes over, and departs from the PAS)